QUANTITATIVE MEASUREMENTS OF RADAR ECHOES FROM AIRCRAFT

R. C. Macdonald
R. D. Stewbridge

ELECTRONICS DIVISION

10 September 1957

NAVAL RESEARCH LABORATORY
Washington, D.C.

QUANTITATIVE MEASUREMENTS OF RADAR ECHOES FROM AIRCRAFT

XIV. FJ-2

By

F. C. Macdonald
R. D. Shewbridge

10 September 1957

Wave Propagation Branch
Electronics Division
Naval Research Laboratory
Washington 25, D. C.

ABSTRACT

Some radar characteristics of the FJ-2 aircraft are described quantitatively for radar frequencies of 115, 215, 1250 and 2813 Mc. The radar area is greater at the lower frequencies (115 and 215 Mc) than at the higher frequencies (1250 and 2813 Mc). Radar areas at 115 Mc tend to be six times as great, and radar areas at 215 Mc tend to be three times as great, as the radar areas at the two higher frequencies. Average values of the radar area over both head and tail aspects are found to be:

115 Mc - 10.0 m^2
215 Mc - 3.2 m^2
1250 Mc - 1.7 m^2
2813 Mc - 1.7 m^2

The probability distributions of single-pulse amplitudes are essentially equal to the probability distributions of median-pulse amplitudes when such medians are obtained from sample times of 8 seconds for 115 Mc, 1/2 second for 215 Mc and 1/12 second for 1250 and 2813 Mc. A comparison between these measurements and model measurements is attempted.

PROBLEM STATUS

This is an interim report on the problem; work continues.

AUTHORIZATION

NRL Problems: R02-06 (NE 050500-20.19)
R02-10 (NR 412-008)
R07-04 (NR 413-003)

Introduction

This is the second of a series of reports on a tactical problem designed by the Office of the Chief of Naval Operations. The first report contained information relating to the F2H-2B aircraft[1]. This report contains information relating to the FJ-2 (Air Force F-86) aircraft.

The purpose of the work described in these reports is to determine the optimum manner (that giving the least chance of detection) in which U.S. aircraft should approach an enemy target guarded by radar. This report, on one phase of this overall problem, allows the computation of the probability of detection of the FJ-2 aircraft by radars operating on several frequencies. Additionally, this report compares these dynamic measurements with model (static) measurements.

The overall measurement program included the F2H-2B, AJ-1, AD-4B and the FJ-2 aircraft.* The aircraft were flown on courses, altitudes, and with flight-attitudes calculated to simulate, as closely as possible, the range of aircraft aspects observed by a ground-based radar with the aircraft at normal combat altitude and speed. Simultaneous measurements were made at radar frequencies of 115, 215, 1250, and 2813 Mc.** Unlike all of the other aircraft that were measured, the FJ-2, whose radar characteristics are described in this report, did not carry external wing tanks or the T-63 shape (simulated Mark VII bomb). It should be pointed out that such attachments can affect the results considerably,

* Although measurements were also requested for the F7U-3 and A3D aircraft, they were not made available for the measurement program.

** These frequencies were the nearest available to the requested frequencies of 73, 200, 1200, and 2860 Mc.

especially at the higher frequencies. If the target aircraft carries a radar antenna, its effect can be particularly important at certain aircraft aspects.

Methods of Measurement

A series of flights was planned so that while the aircraft was between the ranges of 8 and 11 miles from the radar, it would present to the radar a series of nominal aircraft aspects (0°, 5°, 10°, 15°, 20°, 30°, 90°, 180°, 185°, 190°, 195°, 200°, 210°, and 270° in azimuth and 2.3° to 3.2° in elevation). The following azimuths were actually accomplished: 340°, 345°, 350°, 355°, 0°, 5°, 170°, 175°, 180°, 185°. (The data were taken in the 8-11 mile region since here a maximum of the interference pattern occurs for both the 115 and 215 Mc radars and the desired elevation angles of 2.3° to 3.2° could be obtained.) All flights were straight and level at an altitude of 2700 feet. The pilot was instructed to hold the aircraft angle of attack equal to that at normal combat altitude and speed and to hold the requested heading during all of each run (i.e., not necessarily to fly along a particular ground track). With the aircraft flown in this manner, and knowing the range, elevation angle, and azimuth angle to the aircraft from the radar, it was possible to determine a nominal aircraft aspect (defined in Fig. 1). Under these conditions, with an aircraft speed of 250 knots (CAS), the tactical situation of an aircraft at attack speed at 40,000 feet flying against a ground-based search radar at ranges from 100 to 130 nautical miles were simulated.

The radar echoes from the aircraft were recorded photographically by two different methods:

1. A movie camera photographed each A-scope presentation with half-second exposures every second. In addition to revealing the presence of interfering echoes, this record of superimposed A-scope traces gave a compressed version of the echo behavior.

2. The aircraft video echo was gated from the total video and presented on an oscilloscope which was photographed on a continuously moving film. This record permitted a pulse-by-pulse analysis of the echo behavior and is the record from which most of the data in this report are derived.*

In addition to these two records, a data board containing such information as time, range, elevation and bearing of the radar was photographed by a third camera. Timing marks on each film permitted correlation of all records.

Radar area, σ, as used in this report, is defined, if the target is in free space**, by the equation:

$$\sigma = P_R(4\pi)^3 R^4/P_T(G\lambda)^2$$

in which P_R = received power, R = range of the target, P_T = transmitted power, G = antenna gain, and λ = radar wavelength. To convert the received power, P_R, into quantitative values of radar area, σ, the radars were calibrated or "standardized."

* Since previous work had indicated that a sampling of 60 times per second would be adequate for the fluctuation rates of jet aircraft echoes, the pulse-by-pulse recording rate was 60 pulses per second, although the actual radar repetition rate was 120 cycles per second.

** If not in free space (i.e., ground reflected energy reaches the target) this equation is modified by a term depending upon antenna beam shape, height of radar antenna, altitude and range of the target, reflection coefficient of the ground, and radar wavelength.

Two methods of calibration were used in this work. The first of these methods, the method of radar parameters, has been described by M. Katzin.[2] The second method, the standard-target method, requires placing in the field of the radar a target of known radar area (sphere, corner, sheet) and comparing the amplitude of its echo with the aircraft echo. It was possible to use both of these methods at 2813 and 1250 Mc, but only the standard-target method could be used at the two lower frequencies. These methods and their effect upon the accuracy of the data in this report are discussed in Appendix I.

Results

Low Frequencies (115 and 215 Mc):

In the F2H-2B report[1], two prominent features of the low-frequency data were found: (1) The A-scope records contained practically as much information as the pulse-by-pulse records and (2) the radar area varies rather slowly with aircraft aspect. These features were also observed in the low-frequency data taken on the FJ-2 and the analysis of these data was based upon these observations. These two phenomena will probably occur in all cases of jet aircraft in straight and level flight when the radar wavelength is "large."

The A-scope records were read each second for the highest echo which occurred during the half-second the shutter of the camera was open. The pulse-by-pulse records were read, in each corresponding half-second, for both the maximum and the minimum echo. Plots of the 115 and 215 Mc A-scope readings, together with the maximum and minimum pulse-by-pulse values, appear in Fig. 2. Since the A-scope records were read for

the highest echo, the A-scope plot should coincide with the plot of the pulse-by-pulse maximum. Deviations of one from the other are probably due to reading error. It should be pointed out that neither the pulse-by-pulse maximum nor the A-scope value exceeds the median value (which is not plotted) by more than one or two db except in the regions of deep fading. Therefore, the A-scope readings yield almost as much information as the pulse-by-pulse records.

Since only a small amount of data, all in the aspect-region of nose and tail, was recorded on this aircraft, it is not possible to plot radar area as a function of aspect. The low-frequency data are presented in Fig. 3 as a series of plots of A-scope readings versus time, for each flight.

In any particular interval of time, the fraction of the total number of points which lie above a given value of radar area is the probability that the radar area will exceed this value in a single antenna scan if the radar presentation time is equal to or less than one-half second. For longer presentation times, this probability may be obtained in the same way by an appropriate running average of the data. Where several flights contain the same azimuth interval, additional observations of a particular probability may be obtained from each repetition of the aspect interval.

High Frequencies (1250 and 2813 Mc):

Data for these frequencies, taken from pulse-by-pulse records, were analyzed for probability distributions over certain aspect intervals. The data were divided into samples to yield the maximum number of repeats of nominal aircraft-aspect (during the different flights). These samples cover between 10 and 15 seconds in time and span

from 0° to 5° in azimuth. The small amount of data is not continuous over the entire nose and tail regions and only a few repeats occur.

Three things must be considered in choosing sample times and aspect intervals. First, the sample time should not be long compared to the decision time of tactical problems (for a given tactical problem, answers are required at a rate dependent upon such things as target range and speed). Second, the sample time should be long compared to the period of natural oscillation of the aircraft. Third, the aspect interval within a sample should only be reasonably longer than the fluctuations of exact aspect.

The compromises in the reduction of the data for this report were aimed at presenting the most useful and complete data summaries permitted by the finite number of flights and the finite information known about the aircraft-aspect. It should be pointed out that, as a rule, a probability distribution taken over a given nominal aircraft-aspect is not repeatable within a small number of samples. Although the samples are based upon a time which is long compared to the natural lateral oscillation period of the aircraft (1/2 cps), it has been found that nominal aspect* from flight-to-flight may differ as much as ± 6° from the exact aspect. These considerations, especially since random aspect changes have a greater effect at the higher frequencies, have forced a more statistical description of the 2813 and 1250 Mc data.

The results, presented in Tables I and II, show the probability that the value of the radar area equals or

* Nominal aspect is that computed from the presumption of level attitude and compass heading as instructed. Exact aspect is nominal aspect as modified by actual roll, pitch, and yaw of the aircraft.

exceeds certain discrete levels and are taken from pulse-by-pulse data. Although the echo fluctuations at both 1250 and 2813 Mc were much more rapid than those at 115 and 215 Mc, there is practically no variation in signal level during the radar presentation time of 1/12 second used here. Figs. 4-11 show a series of unaccumulated probability distributions. On each figure, the solid curve represents the distribution of single-pulse amplitudes while the dotted curve represents the distribution of median-pulse amplitudes for given presentation times. Note that these two curves for each of the two high frequencies lie very close together, indicating signal stability over the presentation times used.

Frequency Trend

To find a value of radar area, for each given frequency, representative of the entire nose and tail aspects, the median of the medians of all samples for each frequency was determined. There was no appreciable difference between the values for the nose and tail aspects on any frequency and the values show a frequency trend as shown below.

115 Mc; σ = 10.0 m^2
215 Mc; σ = 3.2 m^2
1250 Mc; σ = 1.7 m^2
2813 Mc; σ = 1.7 m^2

A discussion of the day-to-day variations of the readings taken on the standard target, which is found in Appendix I, points out, however, that for this particular day the measured value of the target area is about 2 db above the theoretical value for 2813 Mc and 2 db below on 1250 Mc. This correction has been applied to the values in the above table and to the values used in the next paragraph for comparison with the work of others.

This table indicates that the value of radar area at 115 Mc is 6 times greater than the value at the two high frequencies and three times greater than the value at 215 Mc. No explanation for this frequency trend, noted previously[1], is offered.

Comparison with other Measurements:

Measurements of the radar area of static models of the F-86 have been made by McGill[3] and Ohio State Universities[4]. The McGill measurements of a 1/20 scale model simulated radar frequencies of 200 and 1200 Mc while the Ohio State measurements of a 1/9 scale model simulated a radar frequency of 2600 Mc. The method of measurement, used by both McGill and Ohio State, was to set the model at various elevation angles and take measurements from 0° to 360° in azimuth. Since the elevation angles does not remain constant during a dynamic run, the static measurements at greater and smaller elevation angles are used for comparison with the dynamic measurements.

Figure 12 is a composite plot of McGill, Ohio State, and NRL data. The McGill data (200 and 1200 Mc) are plots of amplitude versus azimuth for each 1° change of azimuth. The Ohio State data (2600 Mc) are plots of the maximum and the median for each 10° change of azimuth. These values are plotted as rectangles bounded at the top by the maximum and at the bottom by the median. The rectangles defined by +++ represent the 0° elevation values while those bounded by solid lines represent the 10° elevation values. The NRL data at

* Although the elevation of the radar was between 2.3° and 3.2° the elevation aspect is the elevation of the radar plus the angle of attack plus a third angle dependent upon the curvature of the earth. The elevation aspect angle for these runs lies between 6° and 8°.

at 215 Mc are plots of amplitude versus azimuth while the 1250 and 2813 Mc data are plots of "maximum-median" rectangles for various azimuth intervals.

No point-by-point comparison is possible due to the different forms in which the data are presented, the lack of data at certain intervals, and differences between the "nominal" aspects of a dynamic run and the "exact" aspects of a static run. Only general observations can be made: The 200-215 Mc data of McGill, at both 5 and 10° elevation, tends to agree with values obtained by NRL (only) at certain points. For the most part the NRL data lies between the two McGill curves. The 1200-1250 Mc NRL data are sometimes above and sometimes below those of McGill at both elevation angles. The 2600-2813 Mc NRL data seems to be consistently higher than the Ohio State data. Every median (except three at the tail aspects) lies above the values obtained by Ohio State at both elevation angles.

The difference between the NRL and Ohio State data has been noted before by Ohio State[5], when they compared other measurements of the F-86[6]. They reported that when the static measurements were less than 1 m^2, the NRL data was about 9 db higher; when the static measurements were between 1 and 10 m^2, NRL data was about 2.4 db higher; and when the static measurements were greater than 10 m^2, the NRL data was about 1.5 db lower. In their discussion of the general problem of comparing static and dynamic runs, Ohio State pointed out that discrepancies may occur because of imperfect modeling of both the aircraft and certain radar parameters, polarization, range, differences in types of recording mechanisms, calibration errors, differences in aspects, differences in frequencies, and receiver noise. They discuss

these problems in detail, and this discussion will not be repeated here.

However, one possible explanation of the differences can be eliminated. The NRL data on both the F-86 and the FJ-2 were not seriously affected by receiver noise. The F-86 medians, at aspects where the difference between the NRL and Ohio State data is large, were 20 db above noise level. All medians on the FJ-2 in the region of large differences are at least 10 and many times 20 db above noise level.

In summary, the NRL data on the FJ-2 are a new and independent set of dynamic measurements which apparently still show the same deviation from the Ohio State model measurements. The lack of dynamic data, especially at identical aspects, has greatly hindered the comparison of data.

Acknowledgements:

The experimental portion of this work was a joint undertaking by the Wave Propagation and Search Radar Branches of the Naval Research Laboratory. The contributions of the Search Radar Branch, Radar Division to this program are gratefully acknowledged.

References

1. Macdonald, F. C., "Quantitative Measurements of Radar Echoes from Aircraft, XIII. F2H-2B." NRL Memorandum Report No. 527, dtd 30 September 1955.

2. Katzin, Martin, "Quantitative Radar Measurements," Proc. of IRE, Vol. 35, No. 11, November 1947.

3. Hay, D. R., "Radar Cross Sections of Aircraft," McGill University Technical Report No. 15, 1 June 1952.

4. Kouyoumjian, R. A., Moranda, P. B., Wright, P., "Echo Measurements of the F-86 Aircraft at 2600 Mc," Ohio State University Data Set No. 7, 10 May 1952.

5. Moranda, P. B., "Comparison of Static and Dynamic Echo Area Measurements," Ohio State University Report No. 475-3, 30 October 1953.

6. Ament, W. S., Macdonald, F. C., Passerini, H. J., "Quantitative Measurements of Radar Echoes from Aircraft, VI. Corrected F-86 Amplitude Distributions and Aspect Dependence," NRL Letter Report C-3460-143A/52 lmp, 15 December 1952.

APPENDIX I

Radar Calibrations

The standard target for the two higher frequencies was a triangular corner reflector (the length from apex to any corner was equal to 2 feet) mounted approximately 25 feet above the water. The standard target for the two lower frequencies was a 10 foot by 10 foot flat screen mounted about 75 feet above the water. Pictures of the targets appear in Figs. 13 and 14.

The radar area of the high frequency standard target, as measured by the radar parameters method during the four operating days, is compared with the theoretical value in Fig. 15. (The height variation is due to tide.) The measured values at 2813 Mc are scattered approximately ± 3 db about the theoretical value* with little relation to target height. The 1250 Mc measurements are correlated with target height but appear about 2 db low with a scatter of approximately ± 1/2 db.

In an attempt to explain the low measured values for the radar area of the triangular target at 1250 Mc, this target was replaced by an 18 inch by 18 inch flat sheet whose radar area was measured (by the radar parameters method) as the sheet was varied in height. The measured and theoretical values of radar area are plotted against height in Fig. 16 and 17. The support for this target was tilted so that the relative phase of any background echo (from the support) should change with target height. The oscillations in the measured values at 1250 Mc may be due to an interfering background echo, but since the peaks of the oscillations are

* For this particular day, values are 2 db above theoretical.

below the theoretical value, the low values of measured radar area are not explained. Other possible causes for the low measured values are deformation of the target, a reflection coefficient of the sea different from -1, or an erroneous measurement of a radar parameter. Without further information it is concluded that the 1250 Mc data in this report are low by a factor lying between 0 and 3 db and believed to be nearer to 2 db.

It is reasonable to assume that the background echo (from the target support) is responsible for the differences between the theoretical and measured curves of Fig. 16 (2813 Mc). Since, in Fig. 17, the background echo at 1250 Mc changes phase by a full cycle about every 4 feet, the same phase change should occur every 1.8 feet at 2813 Mc. The "sampling rate" in Fig. 16 was every 1.5 feet (i.e., the flat sheet was moved in height in increments of 1.5 ft), which is sufficiently close to 1.8 feet to explain the slow cycling between measured and theoretical values. Accordingly, it is concluded that the errors in the 2813 Mc data in this report are small compared with ± 3 db.

The only check on the absolute accuracy of the low-frequency target was computation (for the 215 Mc radar) using measured values of transmitted and received powers and a nominal value of antenna gain. According to this computation is a poor checking procedure (the 3 db difference could be the result of using an incorrect value for nominal antenna gain, a quantity which is squared in the radar area computation) and allows only a negative conclusion: there is no reason to suspect the accuracy of the low frequency data in this report.

The measurements have indicated that the ratio of the radar area at 115 Mc to the radar area at 2813 Mc is about 6 to 1. After applying the estimates of accuracy, it seems equally likely that this ratio is 3 or 4 to 1.

TABLE I

1250 Mc/s

Cumulative Probability (X100) of $A = 10 \log_{10} \sigma$ (σ in square meters) for Azimuth Intervals I (I in degrees) and Sample Size Q (Q in number of pulses). Q/60 = Length of Sample in Seconds

I:	330.7 335.8	335.8 340.0	335.8 340.0	335.8 340.0	335.8 340.0 *	340.0 344.0	340.0 344.0	340.0 344.0 *	344.0 347.0	344.0 347.0
Q:	900	960	660	720		780	840		780	660
A										
18.6			98.9	99.3						
17.6			98.9	99.3						
16.6	98.2		98.3	98.9		100.0				
15.6	97.4		98.0	98.2		99.7	92.3	96.0		
14.6	96.7		97.9	97.5		99.6	91.3	95.4	98.6	
13.6	96.0	99.4	97.0	96.8	97.7	99.4	90.4	94.9	97.4	
12.6	95.1	98.4	96.4	95.5	96.8		89.5		95.8	
11.6	94.0	97.3	95.9	94.6	95.9	98.3	88.6	93.4	94.1	100.0
10.6	92.9	96.3	94.7	93.5	94.8	96.4	87.9	92.1	92.2	99.1
9.6	91.4	94.8	93.9			93.6	85.9	89.7	91.5	98.5
8.6	89.4	93.5	91.8	90.8	92.0	91.3	84.8	88.0	90.5	97.7
7.6	87.7	92.1	86.2	88.7	89.0	87.8	75.4	81.6	89.1	97.3
6.6	85.8	89.5	80.6	86.5	85.5	74.5	76.8	75.6	87.8	96.7
5.6	83.3		72.6	83.7	81.9	63.5	65.1	64.3	86.0	95.7
4.6	79.3	81.0	63.8	82.0	76.6	52.8	62.3	57.5	82.9	80.1
3.6	69.0	74.9	53.5	77.9	68.8	43.6	58.3	50.9	81.3	58.9
2.6	56.0	69.2	42.9	71.1	61.1	31.9	55.0	43.4	79.5	37.7
1.6	48.7	59.2	35.1	63.2	52.5	20.6	51.4	36.0	75.9	17.0
-0.6	41.1	38.2	24.2	46.8	36.4	14.1	46.2	30.1	66.1	11.5
+0.4	32.1	24.8	16.5	29.9	23.7	8.8	43.0	25.9	57.9	7.0
1.4	19.8	15.8	13.8	15.8	15.1	1.4	39.3	20.3	48.1	5.4
2.4	6.8	11.7	12.1	7.9	10.6	0.0	38.4	19.2	41.7	4.7
3.4	2.2	3.3	10.1	4.6	6.0				33.1	4.2
4.4	0.0	0.0	2.1	0.7	0.9		32.6	16.3	20.5	3.6
5.4			0.0	0.0	0.0		30.6	15.3	6.9	2.9
6.4							25.1	12.5	2.3	1.9
7.4							14.2	7.1	0.0	1.5
8.4							4.5	2.2		0.0
9.4							0.0	0.0		

* Denotes average of all data for indicated azimuth interval.

TABLE I
(continued)

I:	344.0 347.0 *	344.9 346.8	347.0 349.4	347.0 349.4	347.0 349.4 *	349.4 351.5	349.4 351.5	349.4 351.5 *	351.5 353.2	351.5 353.2
Q:		720	660	660		840	600		660	600
A										
14.6	99.3									
13.6	98.7									
12.6	97.9									
11.6	97.0						99.5	99.7		
10.6	95.6			100.0	100.0		98.0	99.0		
9.6	95.0	100.0		99.8	99.9		97.7	98.8		
8.6	94.1	98.7		97.7	98.8		96.5	98.2		
7.6	93.2	96.9		94.7	97.3		96.0	98.0		
6.6	92.2	95.1		89.5	94.7		94.8	97.4		
5.6	90.8	92.9		85.0	92.5		91.0	95.5		
4.6	81.5	91.2		80.1	90.0		80.2	90.1		
3.6	70.1	90.1		75.5	87.7		48.7	74.3		
2.6	58.6	87.1		68.2	84.1	100.0	36.3	68.1		
1.6	48.2	79.0		62.0	81.0	98.4	29.2	63.8		
-0.6	38.8	70.1		50.0	75.0	90.7	25.0	57.8		
+0.4	32.4	60.5	100.0	29.5	64.7	78.2	20.3	49.2		
1.4	26.7	52.6	95.9	15.6	55.7	58.9	15.0	36.9	100.0	
2.4	23.3	41.2	89.5	6.5	48.0	40.8	0.3	20.5	93.6	
3.4	18.6	29.0	69.8	0.3	35.0	16.2	0.0	8.1	57.4	100.0
4.4	12.0	24.6	33.8	0.0	16.9	1.9		0.9	33.8	93.5
5.4	4.9	22.5	16.7		8.3	0.0		0.0	27.8	78.3
6.4	2.1	20.4	8.0		4.0				20.5	45.5
7.4	0.7	18.6	0.1		0.0				16.2	23.7
8.4	0.0	14.3	0.0						8.6	8.8
9.4		0.5							0.0	0.2
10.4		0.0								0.0

* Denotes average of all data for indicated azimuth interval.

TABLE I
(continued)

I:	351.5	353.2	357.0	3.8	4.8	171.2	174.5	174.7	174.7	174.7
	353.2	355.4	358.2	4.2	4.8	172.5	175.0	174.7	174.7	174.7
	*									
Q:		1020	840	780	840	900	600	840	900	900
A										
17.6								98.8		
16.6								97.1		
15.6								95.7		
14.6								93.7	99.0	
13.6								91.5	97.2	
12.6								89.4	95.7	
11.6						97.0		88.1	93.2	98.1
10.6						96.1		86.3	89.1	94.9
9.6					70.3	94.3		84.2	85.3	91.1
8.6					66.3	94.0		81.9		84.8
7.6					62.8	93.0		78.8	81.0	72.3
6.6					55.7	92.2		75.5	78.7	55.8
5.6				99.5	53.5	91.0		72.4	77.3	41.1
4.6				96.8	49.5	89.2		70.7	75.3	32.4
3.6				93.2	47.1	86.2		69.0	71.3	26.2
2.6			100.0	90.9	42.5	80.1		65.0	68.8	22.2
1.6			98.6	84.0	41.3	70.6		58.9	67.3	20.1
-0.6			90.0	69.4	39.8	58.8		52.9	65.0	18.1
+0.4			82.5	63.5	38.6	44.5		40.1	58.8	16.1
1.4	100.0	100.0	68.9	50.0	35.4	30.0	100.0	30.3	44.9	13.1
2.4	96.8	99.3	58.7	25.4	21.3	23.3	98.2	22.6	27.7	10.0
3.4	78.7	94.0	44.6	11.7	13.9	15.1	78.4	17.0	18.8	6.9
4.4	63.6	83.9	29.6	1.3	5.4	10.8	52.9	9.4	10.5	2.5
5.4	53.0	64.2	12.0	0.0	0.7	9.5	26.8	0.8	3.1	0.0
6.4	33.0	46.6	6.9		0.0	7.6	1.0	0.0	0.1	
7.4	24.9	29.4	0.0			3.4	0.0		0.0	
8.4	8.7	7.9				0.5				
9.4	0.1	0.0				0.0				
10.4	0.0									

* Denotes average of all data for indicated azimuth interval.

TABLE I
(continued)

I:	174.7	174.7	179.6	179.6	184.5	184.5	184.5	184.5	187.8	188.1
	174.7	175.0	179.7	179.9	184.5	184.5	184.5	185.5	187.9	188.3
	*							*		
Q:		660	960	660	1080	1140	1140		900	900
A										
17.6				99.5	96.9			99.0		
16.6				98.5	96.5			98.8		
15.6				97.3	95.5			98.5		
14.6				95.7	94.7			98.2		
13.6				93.0	92.8			97.6		
12.6				89.7	90.5			96.8		
11.6	93.1			86.7	85.2			95.1		
10.6	90.1			79.4	83.4			94.5		
9.6	86.9	86.2		67.4	81.9			94.0	100.0	100.0
8.6		83.2		64.4	76.5			92.2	99.9	98.9
7.6	77.4	75.2		62.0	73.8			91.3	99.0	95.4
6.6	70.0	60.2		59.1	71.6			90.5	95.7	91.4
5.6	63.6	50.3		56.2	67.1			89.0	85.0	85.4
4.6	59.5	42.6	100.0	50.4	64.2			88.1	70.0	78.9
3.6	55.5	36.5		47.1	61.5			87.2	55.5	73.1
2.6	52.0	31.7	98.4	43.9	59.2			86.4	48.2	68.3
1.6	48.8		84.6	31.3	54.6		100.0	84.9	42.5	63.0
-0.6	45.3	28.6	69.5	20.4	48.1		99.1	82.4	40.8	55.0
+0.4	38.3	8.0	59.7	15.5	43.1	100.0	99.1	80.7	37.2	41.9
1.4	29.4	0.0	48.2	9.4	37.9	99.1	80.3	72.4	33.0	26.2
2.4	20.1		35.8	3.3	31.1	97.1	70.3	66.2	30.2	14.5
3.4	14.2		24.5	0.0	25.0	88.6	58.1	57.2	23.3	3.7
4.4	7.5		14.8		20.7	70.2	51.0	47.3	13.4	0.2
5.4	1.3		8.0		14.2	41.0	41.1	32.1	3.2	0.0
6.4	0.0		5.8		8.0	21.2	28.1	19.1	0.0	
7.4			0.7		4.4	8.6	4.4	5.8		
8.4			0.0		1.2	2.5	0.0	1.2		
9.4					0.0	0.0		0.0		

* Denotes average of all data for indicated azimuth interval.

TABLE II

2813 Mc/s

Cumulative Probability (X100) of $A = 10 \log_{10} \sigma$
(σ in square meters) for Azimuth Intervals I (I in degrees) and Sample Size Q (Q in number of pulses). Q/60 = Length of Sample in Seconds

I:	335.8 340.0	335.8 340.0	335.8 340.0	340.0 344.0	340.0 344.0	340.0 344.0	344.0 347.0	344.0 347.0	344.0 347.0	347.0 349.4
			*			*			*	
Q:	660	720		780	840		780	720		660
A										
19.2	100.0	99.4	99.7							
18.1	99.8	99.4	99.6							
17.0	99.7	99.3	99.5	97.2	98.8	98.0				
15.8	99.7	99.3	99.5	96.3	98.2	97.2				
14.7	99.4	99.0	99.2	95.4	97.4	96.4	98.2	98.9	98.5	
13.6	99.4	98.6	99.0	93.8	96.2	95.0	96.9	98.6	97.7	98.5
12.5	99.4	98.0	98.7	91.7	95.3	93.5	96.3	98.3	97.3	97.7
11.3	99.1	97.8	98.4	89.6	94.4	92.0	94.9	97.8	96.3	96.2
10.2	98.5	97.1	97.8	87.6	92.9	90.2	93.7	96.5	95.1	95.3
9.1	97.9	94.7	96.3	86.0	91.2	88.6	92.7	9555	94.1	93.3
8.0	96.4	90.1	93.2	82.8	89.5	86.1	90.3	93.9	92.1	89.7
6.8	94.2	84.7	89.4	77.5	87.3	82.4	88.1	91.0	89.5	84.5
5.7	91.5	79.0	85.2	72.0	85.6	78.8	86.4	87.5	86.9	77.7
4.5	89.5	73.3	81.4	65.5	82.0	73.7	84.0	84.6	84.3	65.4
3.4	84.8	69.2	77.0	60.5	79.5	70.0	82.3	80.4	81.3	52.3
2.3	81.4	62.0	71.7	54.4	75.6	65.0	78.7	71.8	75.2	41.2
1.2	75.8	56.4	66.1	47.0	70.1	58.5	74.5	62.5	68.5	30.1
-0.1	67.4	49.2	58.3	39.5	63.4	51.4	68.5	57.5	63.0	22.4
+1.0	55.3	42.4	48.8	32.4	56.9	44.6	60.2	51.7	55.9	16.2
2.2	40.9	35.5	38.2	24.9	51.7	38.3	50.5	45.7	48.1	10.4
3.3	27.9	27.5	27.7	17.0	44.2	30.6	43.7	38.5	41.1	6.1
4.4	21.1	19.2	20.1	10.5	30.7	20.6	35.4	31.1	33.2	2.9
5.5	13.9	12.9	13.4	3.7	15.0	9.3	27.8	21.9	24.8	1.2
6.7	5.8	5.7	5.7	1.9	7.9	4.9	16.7	10.4	13.5	0.6
7.8	3.2	2.1	2.6	0.0	5.1	2.5	10.1	4.7	7.4	0.0
8.9	0.0	0.0	0.0		3.0	1.5	3.6	0.7	2.1	
10.0					0.1	0.0	0.0	0.0	0.0	
11.2					0.0					

* Denotes average of all data for indicated azimuth interval.

TABLE II
(continued)

I:	347.0 349.4	347.0 349.4	349.4 351.5	349.4 351.5	349.4 351.5	351.5 353.2	351.5 353.2	351.5 353.2	353.2 355.5	353.2 355.5
Q:	660	*	840	600	*	600	600	*	1200	840
A										
13.6	96.4	97.4								
12.6	96.1	96.9		96.0						
11.3	94.2	95.2	91.9	93.5	93.7					
10.2	93.2	94.2	88.3	91.2	89.7	94.3		97.1		
9.1	91.8	92.5	83.8	87.8	85.8	93.7		96.8		97.0
8.0	89.4	89.5	79.2	84.2	81.7	92.7	100.0	96.3		94.0
6.8	87.3	85.9	74.2	80.5	77.3	92.0	99.8	95.9	96.1	90.7
5.7	83.8	80.7	68.6	78.3	73.4	91.5	99.8	95.6	93.4	86.9
4.5	78.5	71.9	62.3	73.5	67.9	90.3	98.2	94.2	91.6	83.0
3.4	75.8	64.0	53.7	68.3	61.0	89.0	97.5	93.2	89.5	78.0
2.3	72.0	56.6	46.4	65.2	55.8	86.0	96.3	91.1	85.2	71.4
1.2	66.1	48.1	39.2	58.3	48.7	83.5	94.6	89.0	81.4	64.8
-0.1	58.8	40.6	33.9	50.6	42.2	80.0	88.7	84.3	78.0	54.8
+1.0	53.9	35.0	29.4	44.0	36.7	74.5	73.8	74.1	73.2	46.8
2.2	46.8	28.6	25.6	36.5	31.0	70.5	67.3	68.9	68.6	38.3
3.3	38.3	22.2		31.3		61.7	55.3	58.5	64.3	31.4
4.4	34.2	18.5	14.4	29.8	22.1	54.5	48.0	51.2	54.5	25.6
5.5	29.2	15.2	9.9	27.7	18.8	46.7	30.8	38.7	47.4	21.2
6.7	20.3	10.4	7.6	25.2	16.4	36.8	19.3	28.0	43.3	18.0
7.8	12.1	6.0	4.9	22.5	13.7	21.7	12.5	17.1	38.0	15.2
8.9	8.8	4.4	0.1	14.5	7.3	7.2	4.5	5.8	30.0	12.3
10.0	4.8	2.4	0.0	5.3	2.6	0.0	0.0	0.0	23.5	7.8
11.2	3.9	1.9		0.0	0.0				11.0	5.8
12.3	2.3	1.1							4.2	2.5
13.4	0.1	0.0							1.9	0.1
14.5	0.0								0.3	0.0
15.7									0.0	

* Denotes average of all data for indicated azimuth interval.

TABLE II
(continued)

I:	353.2	353.2	355.5	355.5	355.5	355.5	359.4	0.0	3.8	4.4
	355.5	355.5 *	356.3	357.7	357.7	357.7 *	360.0	0.6	4.2	4.6
Q:	1020		600	1200	1380		720	720	780	900
A										
8.0							99.9			
6.8		95.6		96.7		98.3	99.2			100.0
5.7		93.4		94.9		97.4	98.5			99.4
4.5		91.5		93.8		96.9	97.2			98.1
3.4		89.2		92.7		96.3	95.5			95.7
2.3		85.5	100.0	91.2		95.6	93.3			93.8
1.2		82.1	99.8	88.9		94.4	90.7	100.0		91.7
-0.1		77.6	99.5	82.7		91.3	88.3	99.6		88.5
+1.0		73.3	98.5	76.4		88.2	84.8	99.0	100.0	83.0
2.2		69.0	97.2	66.3		83.1	79.3	97.1	99.7	69.4
3.3	100.0	65.2	95.7	56.8		78.4	72.5	95.1	94.5	53.8
4.4	99.4	59.8	94.2	47.1	100.0	73.5	56.0	93.9	80.2	36.7
5.5	94.0	54.2	91.2	37.1	97.1	67.1	40.0	92.1	61.8	22.4
6.7	87.9	49.7	84.5	28.2	91.1	59.6	21.5	81.1	42.6	13.5
7.8	79.7	44.3	63.5	23.8	79.0	51.4	13.2	61.2	23.1	4.4
8.9	72.2	38.2	47.7	18.8	62.7	40.7	5.0	42.2	5.9	0.5
10.0	42.8	24.7	28.7	12.8	47.5	30.1	0.3	27.3	0.1	0.0
11.2	22.1	13.0	13.2	7.7	30.6	19.1	0.0	6.1	0.0	
12.3	9.5	5.4	2.8	7.2	14.1	10.6		0.0		
13.4	2.8	1.6	0.5	5.7	5.0	5.3				
14.5	0.6	0.3	0.0	3.0	0.0	1.5				
15.7	0.0	0.0		0.0		0.0				

* Denotes average of all data for indicated azimuth interval.

TABLE II
(continued)

I:	4.7	4.7	4.8	174.7	174.7	174.7	174.7	174.7	176.0	176.6
	4.7	4.8	4.8	174.7	174.7	174.7	174.7	175.0	176.6	177.2
							*			
Q:	960	900	840	780	900	900		660	900	900
A										
11.3				100.0			100.0			
10.2				99.9			99.9			
9.1				99.9			99.9			
8.0		98.5	100.0	99.6			99.9		91.0	
6.8	98.2	98.0	99.9	99.0			99.7		88.3	
5.7	97.8	97.0	99.4	97.3	100.0		99.1		85.8	61.9
4.5	97.3	95.9	99.2	95.8	99.9	100.0	98.6		82.2	55.1
3.4	96.0	94.8	97.4	92.7	99.7	99.7	97.4		78.8	50.3
2.3	94.6	93.7	92.4	88.6	98.8	98.5	95.3		75.2	43.8
1.2	93.7	91.1	86.3	84.5	97.2	97.4	93.0		71.8	33.4
-0.1	92.4	89.0	84.6	81.5	93.7	94.0	89.7	100.0	68.5	25.3
+1.0	90.1	87.2	83.0	78.3	89.1	89.5	85.6	99.8	65.5	19.7
2.2	88.1	83.0	80.8	70.8	82.5	81.8	78.4	93.9	62.3	12.4
3.3	82.6	69.4	77.5	67.9	75.5	73.9	72.4		56.5	7.0
4.4	73.8	58.7	71.7	64.5	66.8	64.1	65.1	82.6	49.1	0.7
5.5	65.2	47.5	60.8	58.2	52.8	54.4	55.1	70.1	32.8	0.0
6.7	56.7	37.1	50.5	50.9	29.3	45.5	41.9	56.5	21.8	
7.8	47.7	26.3	44.8	43.6	12.2	30.4	28.7	45.6	12.5	
8.9	36.3	18.1	35.8	34.1	3.3	14.4	17.3	27.7	6.5	
10.0	21.8	6.5	27.6	17.7	0.0	6.8	8.2	4.5	3.8	
11.2	15.2	0.7	17.5	7.3		3.3	3.5	0.0	0.3	
12.3	9.6	0.0	8.0	0.1		2.1	0.7		0.1	
13.4	6.2		1.5	0.0		0.3	0.1		0.0	
14.5	0.0		0.0			0.0	0.0			

* Denotes average of all data for indicated azimuth interval.

TABLE II
(continued)

I:	179.6 179.7	179.7	179.7	179.7 179.7	179.6 179.9	184.5 184.5	184.5	184.5	184.5	184.5 184.5
Q:	960	840	900	*	660	1080	1140	1140	720	*
A										
6.8		100.0								
5.7		98.9	99.9	99.4						
4.5		96.9	98.7	97.8						
3.4		92.3	95.5	93.9						
2.3		85.9	93.8	89.8						
1.2		80.8	93.1	86.9						
-0.1		69.5	92.0	80.7		100.0				100.0
+1.0		58.0	89.8	73.9	100.0	99.9				99.9
2.2		50.5	88.1	69.3	99.8	99.1				99.8
3.3		45.6	86.4	66.0	99.1	94.7				98.7
4.4		39.4	83.9	61.6	96.5	84.7	100.0		100.0	96.2
5.5		32.3	80.9	56.6	89.8	70.5	98.1	100.0	99.6	92.0
6.7	100.0	27.4	75.3	51.3	70.4	57.2	94.9	96.0	90.1	84.5
7.8	99.9	21.8	62.1	41.9	53.5	41.8	90.3	77.8	75.1	71.2
8,9	99.1	15.4	40.1	27.7	36.2	28.9	78.1	49.0	68.6	56.1
10.0	87.1	11.1	16.9	14.0	18.5	17.8	55.9	31.9	48.5	38.5
11.2	70.9	9.0	0.3	4.6	7.6	11.4	32.7	17.2	28.2	22.4
12.3	56.6	7.6	0.0	3.8	2.0	6.2	17.1	3.7	16.1	10.8
13.4	40.0	6.1		3.0	0.0		5.0	0.0	4.2	2.3
14.5	22.3	4.6		2.3			0.0		0.0	0.0
15.7	4.4	3.6		1.8						
16.7	0.7	0.0		0.0						
17.9	0.0									

* Denotes average of all data for indicated azimuth interval.

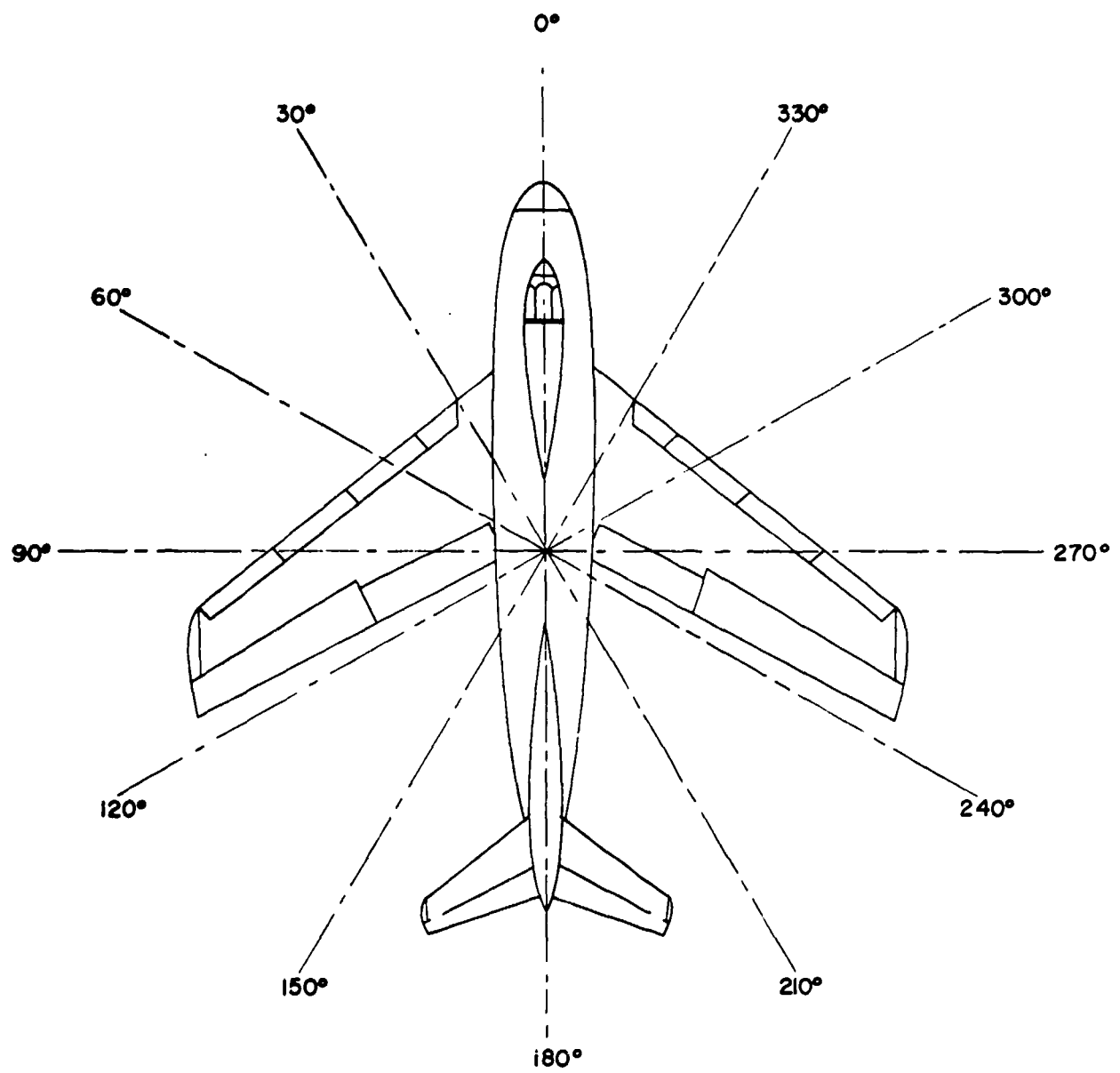

AZIMUTH ASPECT

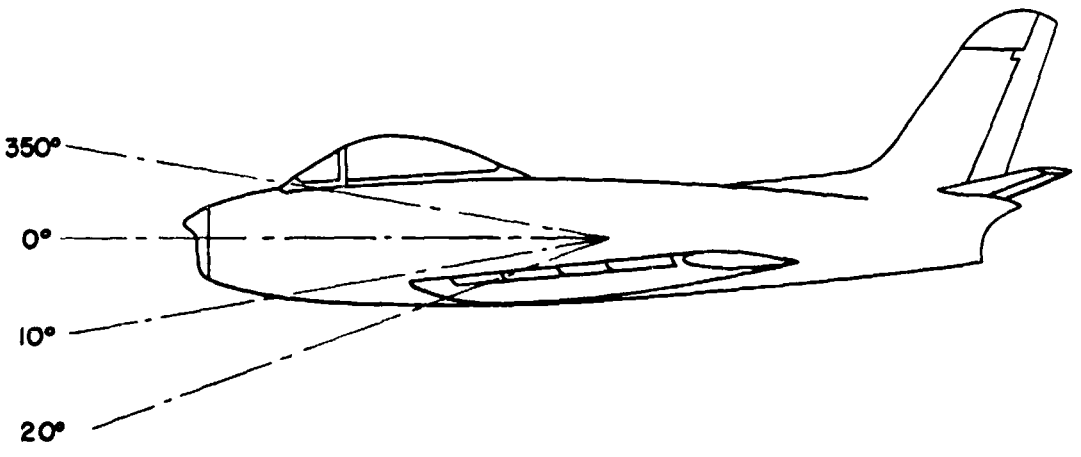

ELEVATION ASPECT

DEFINITION OF ASPECT ANGLES

Figure 1

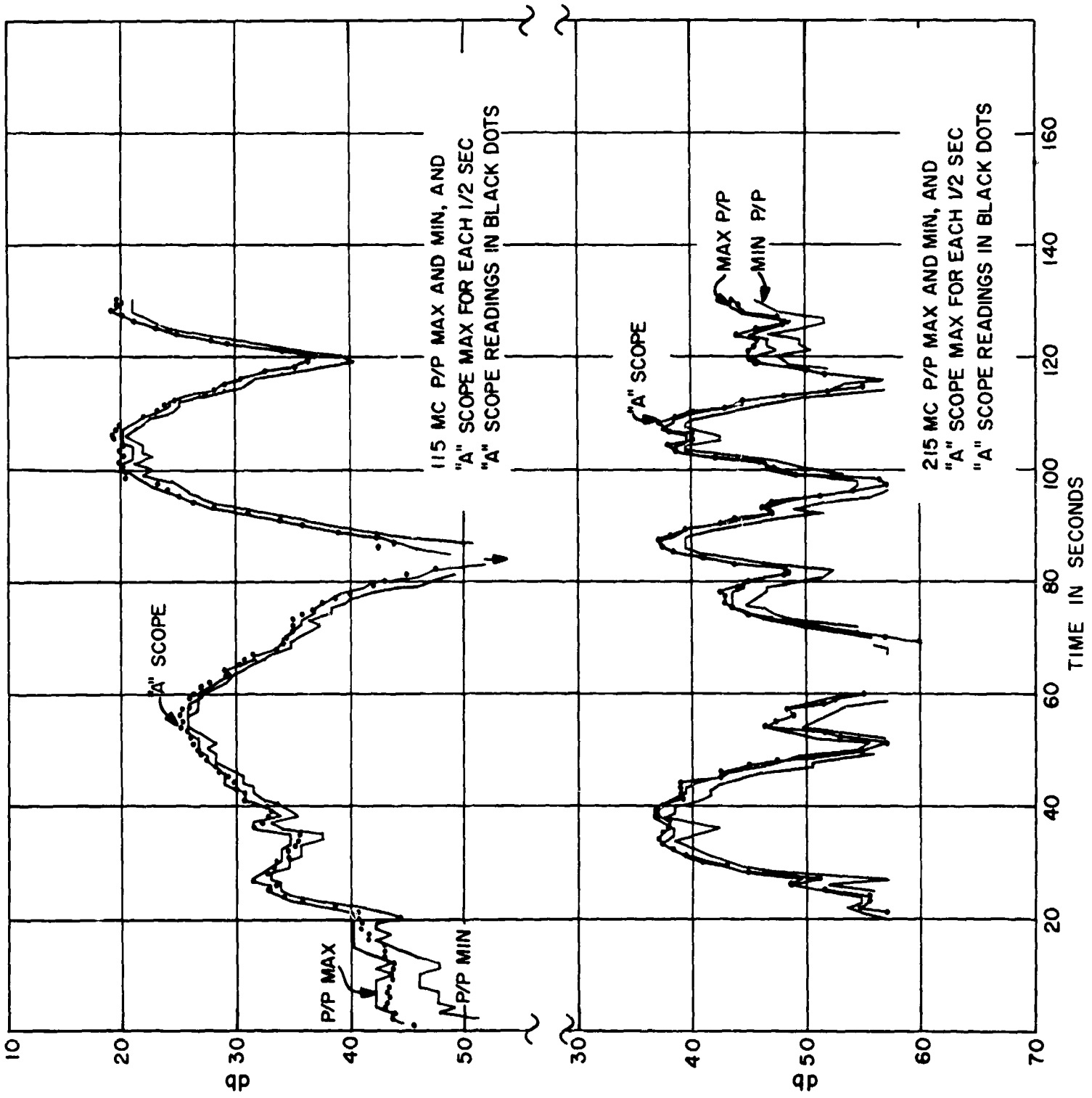
115 MC P/P MAX AND MIN, AND
"A" SCOPE MAX FOR EACH 1/2 SEC
"A" SCOPE READINGS IN BLACK DOTS
"A" SCOPE
P/P MAX
P/P MIN
215 MC P/P MAX AND MIN, AND
"A" SCOPE MAX FOR EACH 1/2 SEC
"A" SCOPE READINGS IN BLACK DOTS
"A" SCOPE
MAX P/P
MIN P/P
db
TIME IN SECONDS

Figure 2

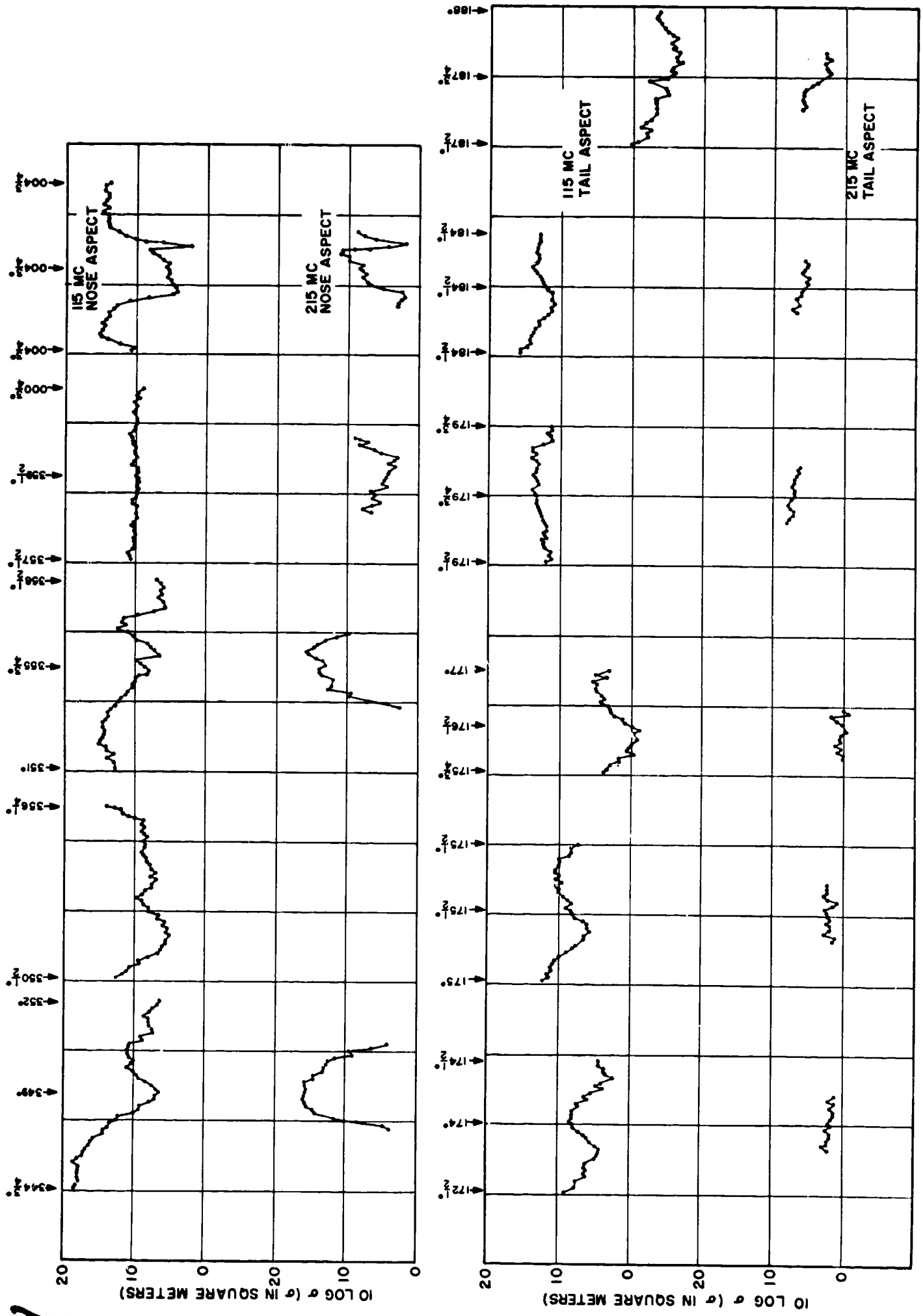

Figure 3

CONFIDENTIAL

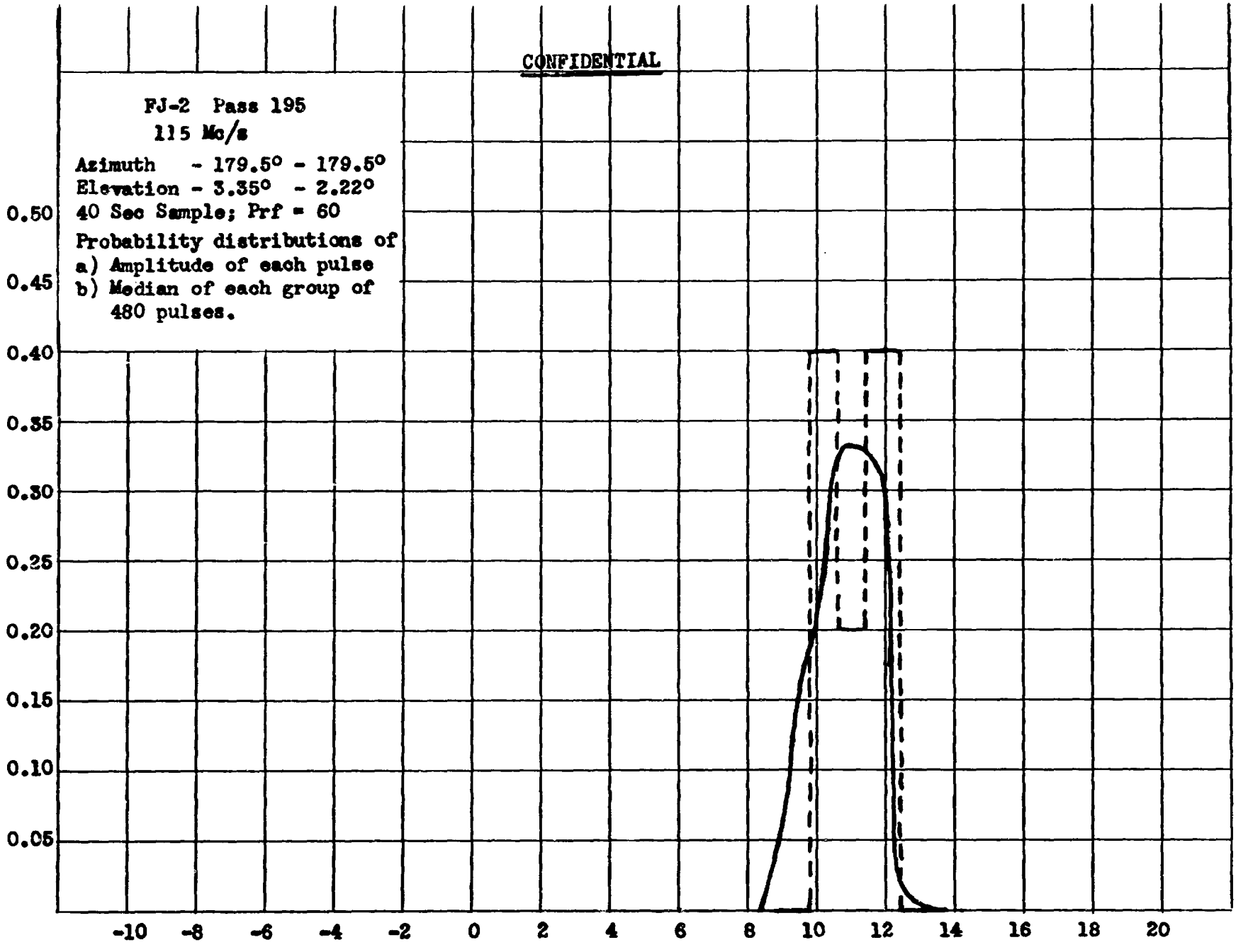

Figure 4

CONFIDENTIAL

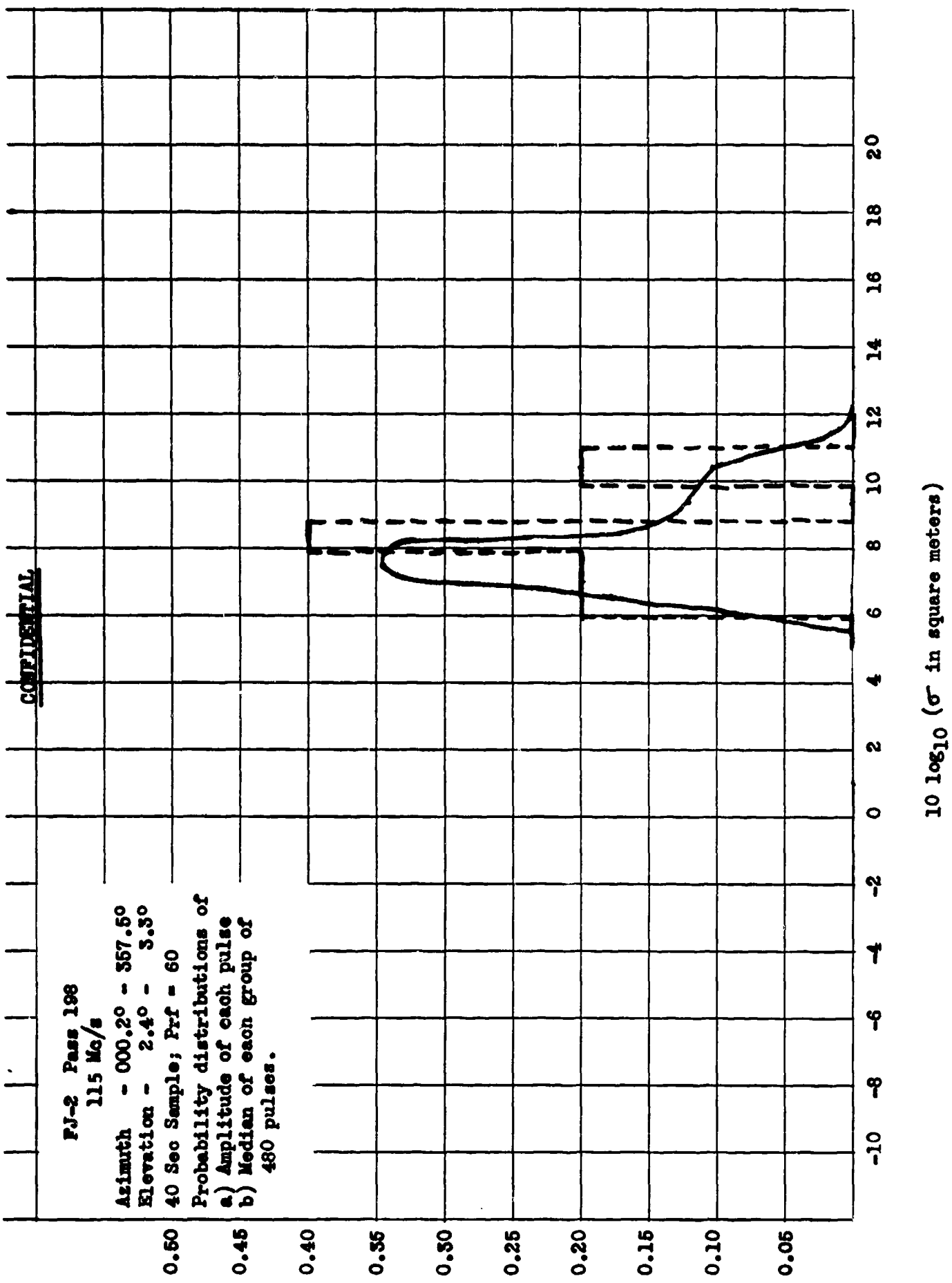

Figure 5

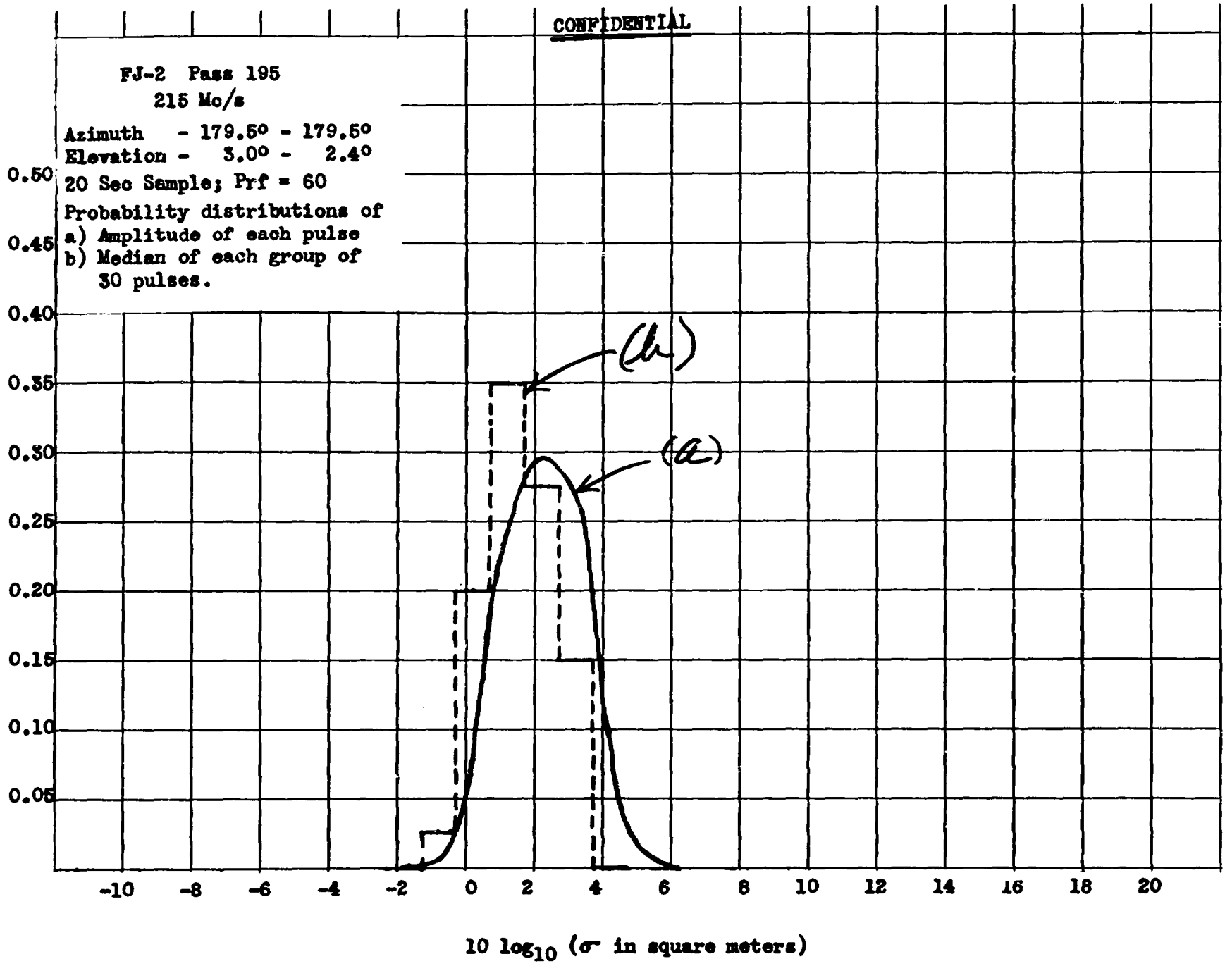
FJ-2 Pass 195
215 Mc/s
Azimuth - 179.5° - 179.5°
Elevation - 3.0° - 2.4°
20 Sec Sample; Prf = 60
Probability distributions of
a) Amplitude of each pulse
b) Median of each group of 30 pulses.
(b)
(a)
Probability of Occurrence
0.50
0.45
0.40
0.35
0.30
0.25
0.20
0.15
0.10
0.05
-10
-8
-6
-4
-2
0
2
4
6
8
10
12
14
16
18
20
10 log10 (σ in square meters)

Figure 6

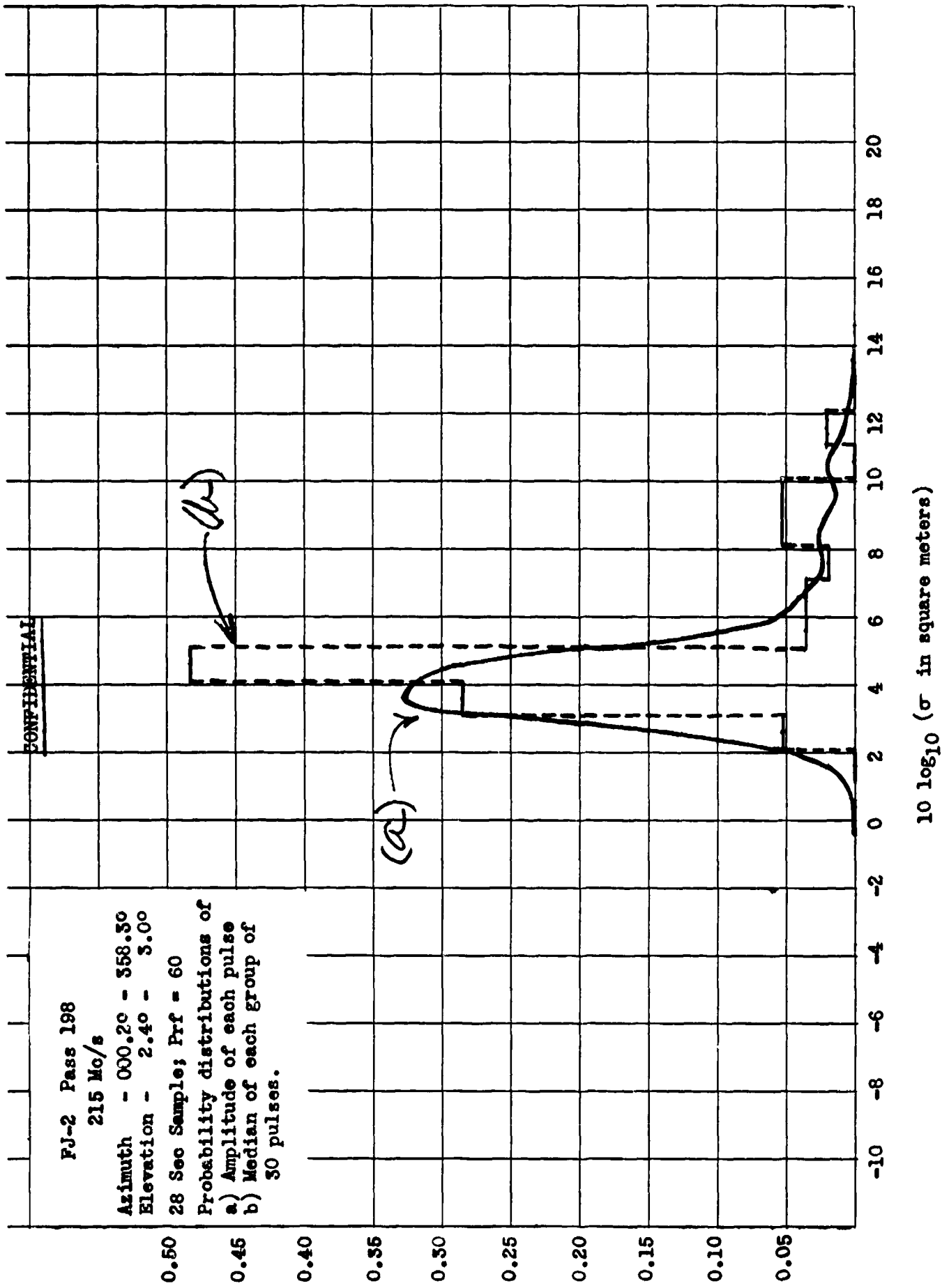
FJ-2 Pass 198
215 Mc/s
Azimuth - 000.2° - 358.3°
Elevation - 2.4° - 3.0°
28 Sec Sample; Prf = 60
Probability distributions of
a) Amplitude of each pulse
b) Median of each group of
30 pulses.
(a)
(b)
CONFIDENTIAL
Probability of Occurrence
0.50
0.45
0.40
0.35
0.30
0.25
0.20
0.15
0.10
0.05
-10
-8
-6
-4
-2
0
2
4
6
8
10
12
14
16
18
20
10 log10 (σ in square meters)

Figure 7

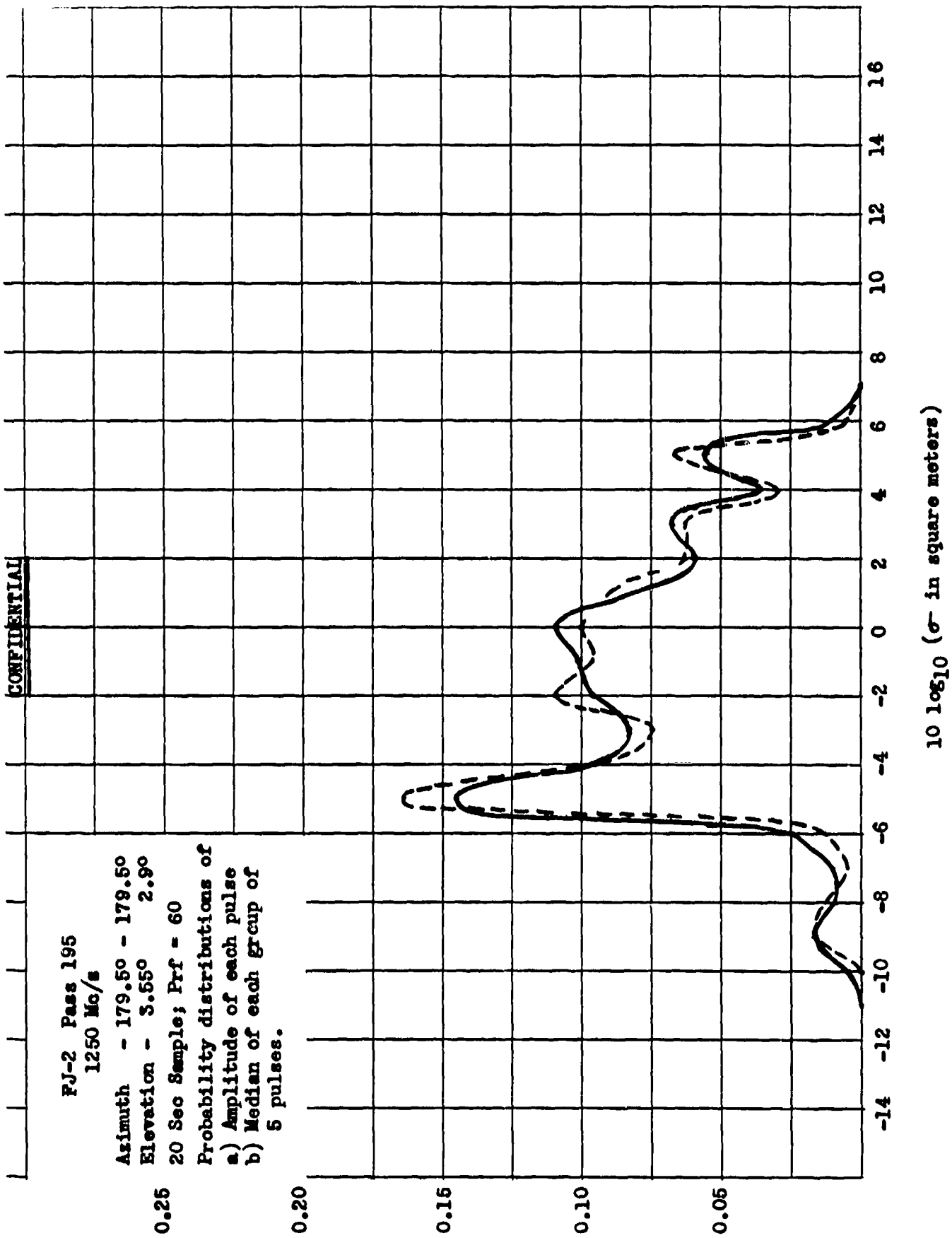
CONFIDENTIAL
PJ-2 Pass 195
1250 Mc/s
Azimuth - 179.5° - 179.5°
Elevation - 3.55° 2.9°
20 Sec Sample; Prf = 60
Probability distributions of
a) Amplitude of each pulse
b) Median of each group of
5 pulses.
Probability of Occurrence
0.25
0.20
0.15
0.10
0.05
-14 -12 -10 -8 -6 -4 -2 0 2 4 6 8 10 12 14 16
10 log10 (σ in square meters)

Figure 8

CONFIDENTIAL

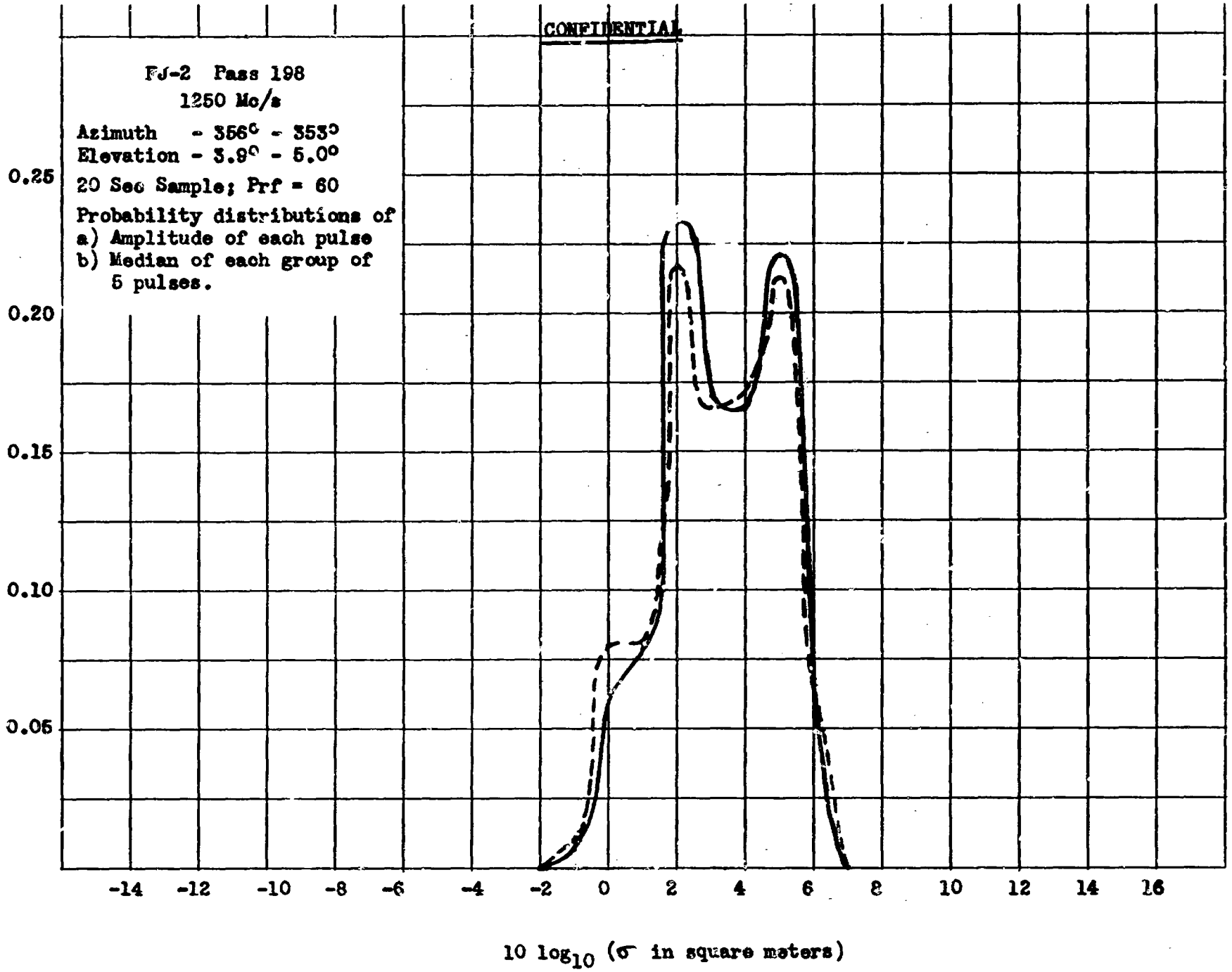

Figure 9

CONFIDENTIAL

CONFIDENTIAL

FJ-2 Pass 195
2813 Mc/s
Azimuth - 179.5° - 179.5°
Elevation - 3.55° - 2.9°
20 Sec Sample; Prf = 60
Probability distributions of
a) Amplitude of each pulse
b) Median of each group of 5 pulses.

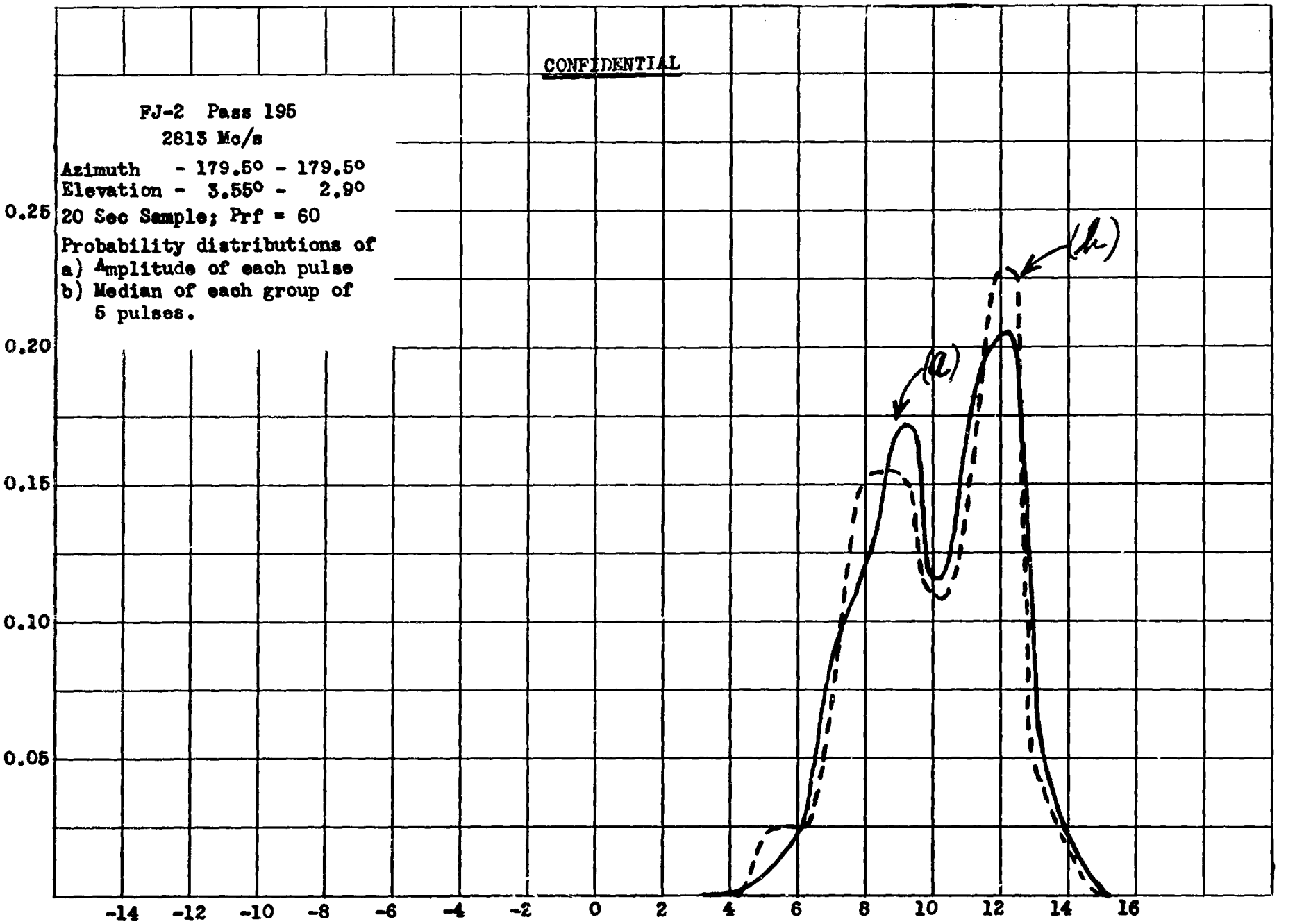

Figure 10

CONFIDENTIAL

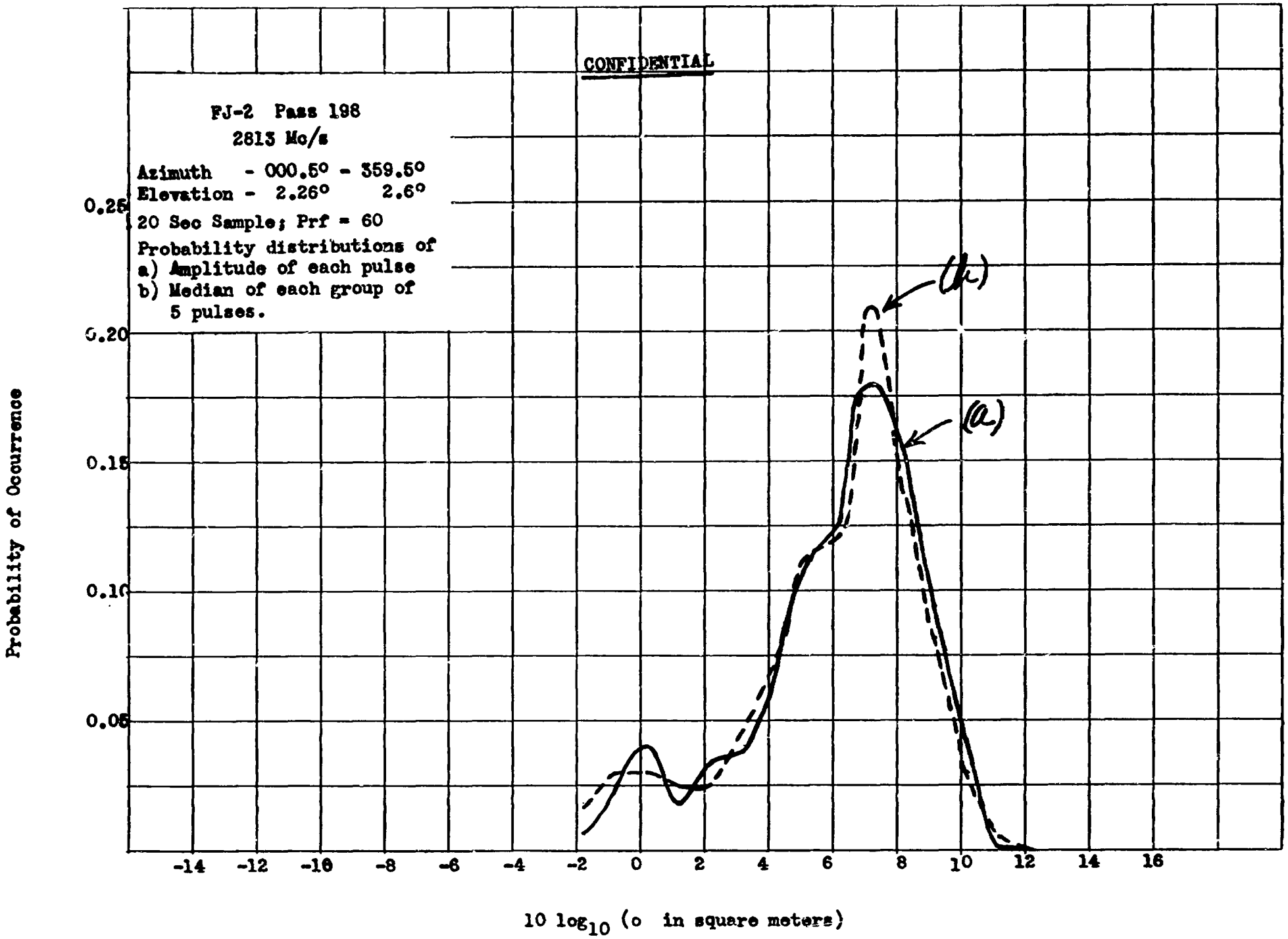

Figure 11

CONFIDENTIAL

COMPARISON OF FJ-2 TO F86

McGILL UNIVERSITY F-86 200 MC/S o-o-o AND •-•-•
NRL FJ-2 215 MC/S ⊗-⊗-⊗

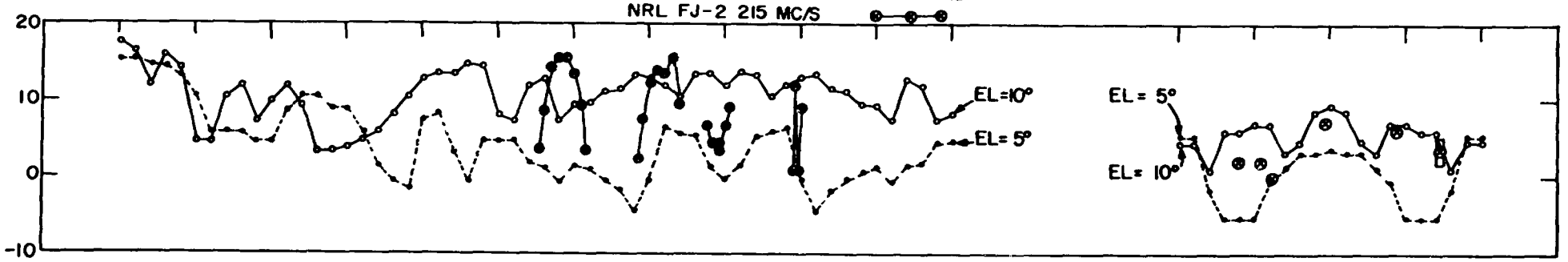

McGILL UNIVERSITY F-86 1200 MC/S o-o-o AND •-•-•
NRL FJ-2 1250 MC/S ▭

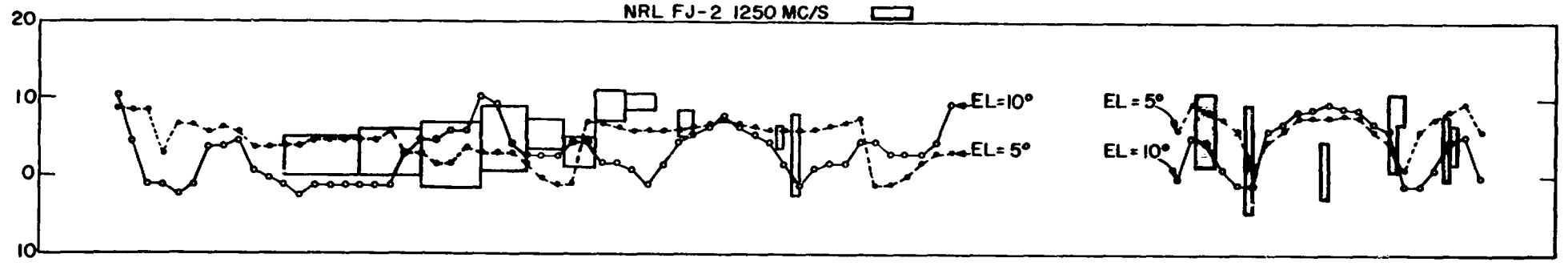

10 LOG σ (σ IN SQUARE METERS)

OHIO STATE UNIVERSITY F-86 2600 MC/S ▭ AND ++++
NRL 2813 MC/S ▭

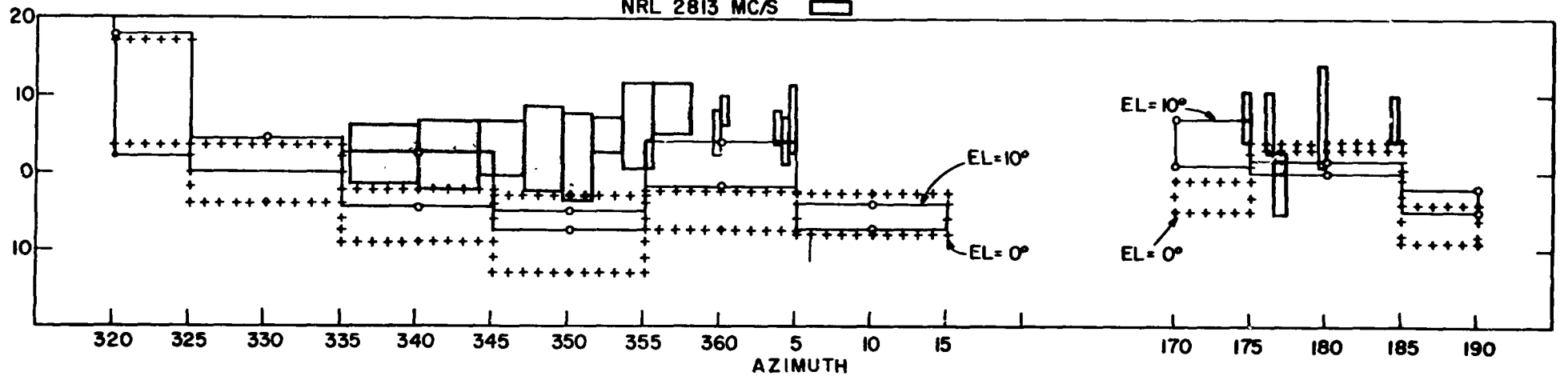

Figure 12

CONFIDENTIAL

Figure 13

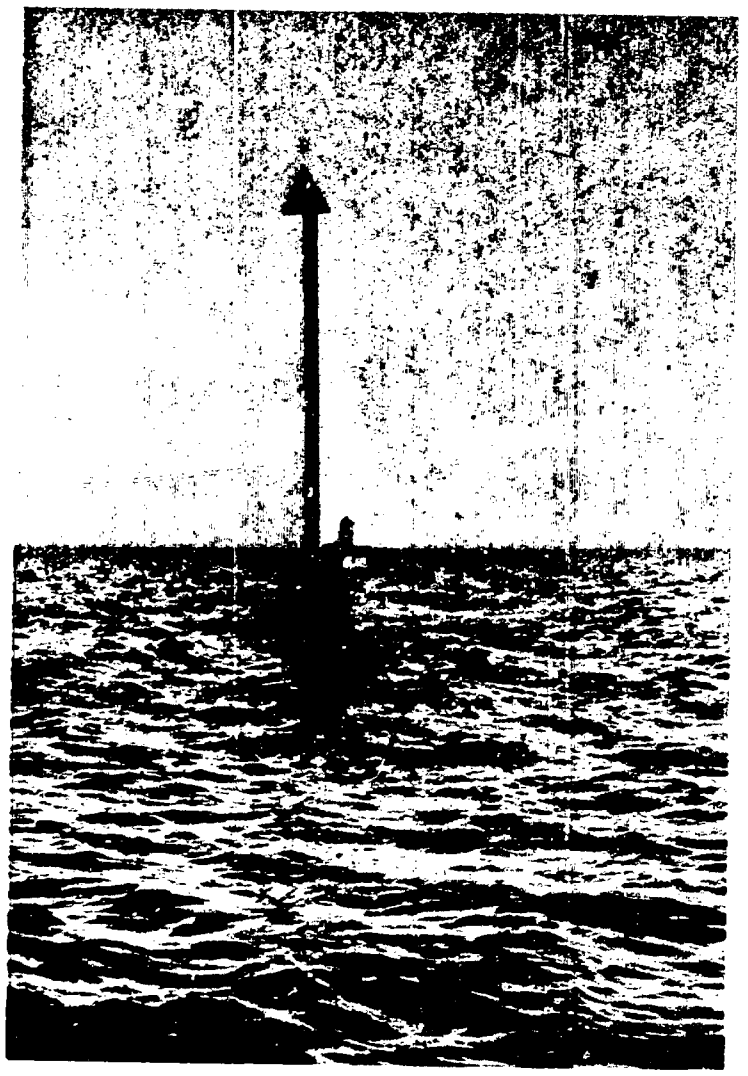

Figure 14

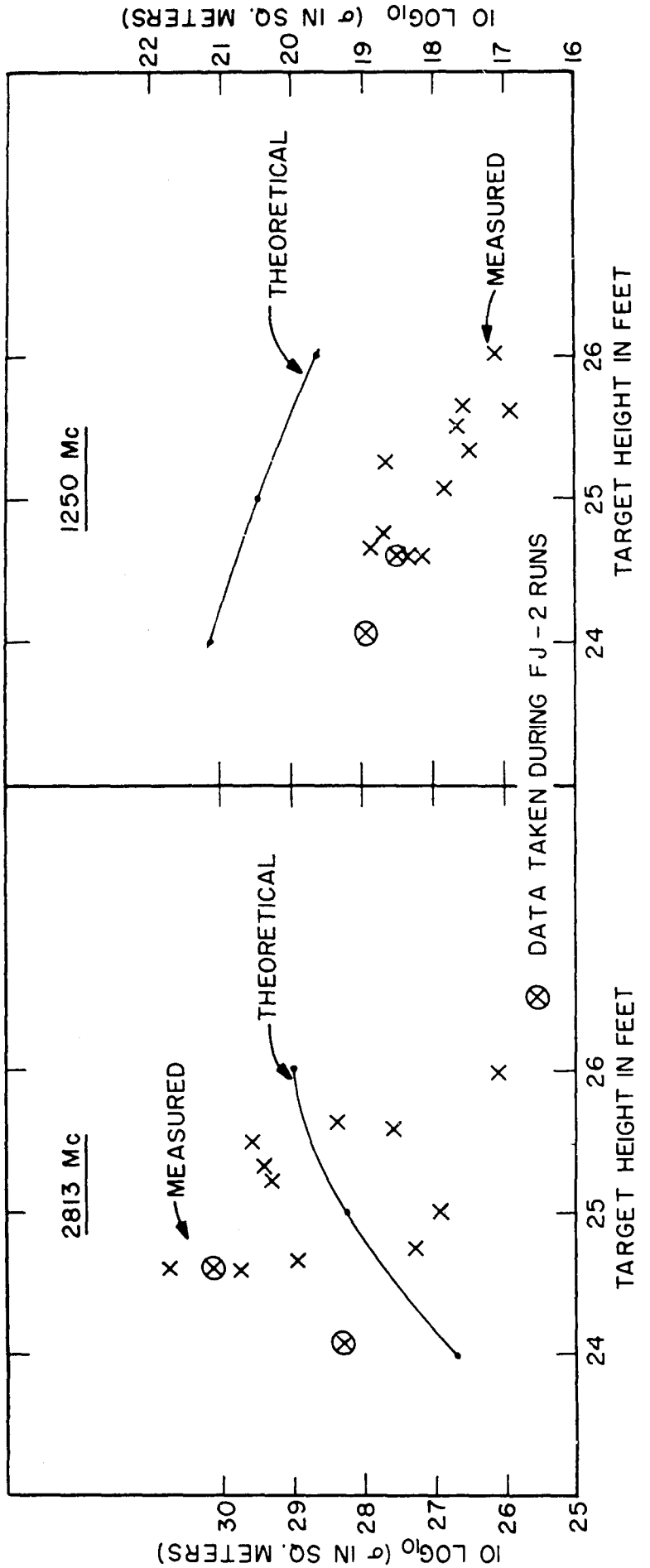
10 LOG10 (σ IN SQ. METERS)
22
21
20
19
18
17
16
1250 Mc
THEORETICAL
MEASURED
26
25
24
TARGET HEIGHT IN FEET
⊗ DATA TAKEN DURING FJ-2 RUNS
2813 Mc
THEORETICAL
MEASURED
26
25
24
TARGET HEIGHT IN FEET
10 LOG10 (σ IN SQ. METERS)
30
29
28
27
26
25

Figure 15

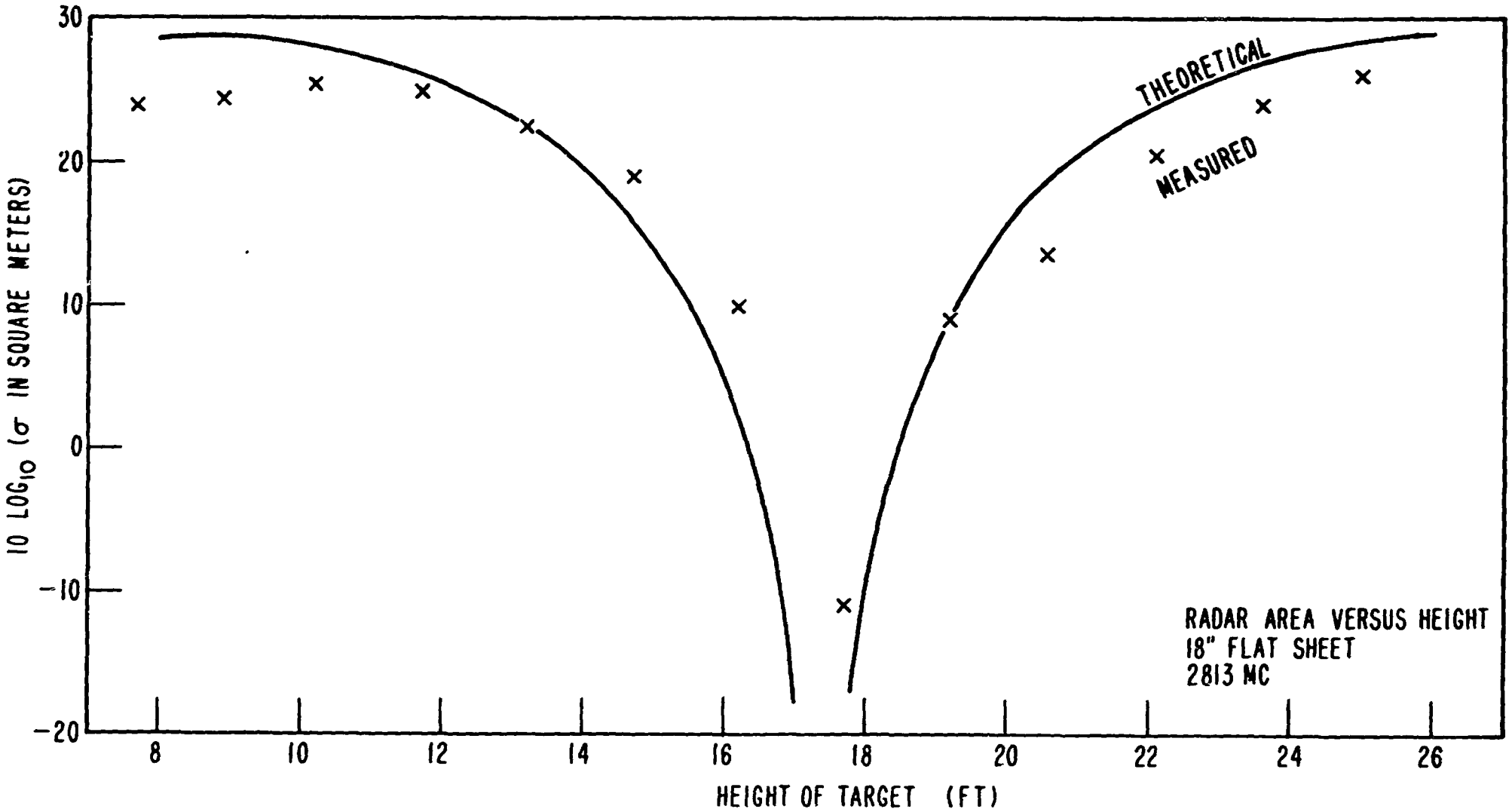
30
20
10
0
−10
−20
10 LOG10 (σ IN SQUARE METERS)
8
10
12
14
16
18
20
22
24
26
HEIGHT OF TARGET (FT)
THEORETICAL
MEASURED
RADAR AREA VERSUS HEIGHT
18" FLAT SHEET
2813 MC

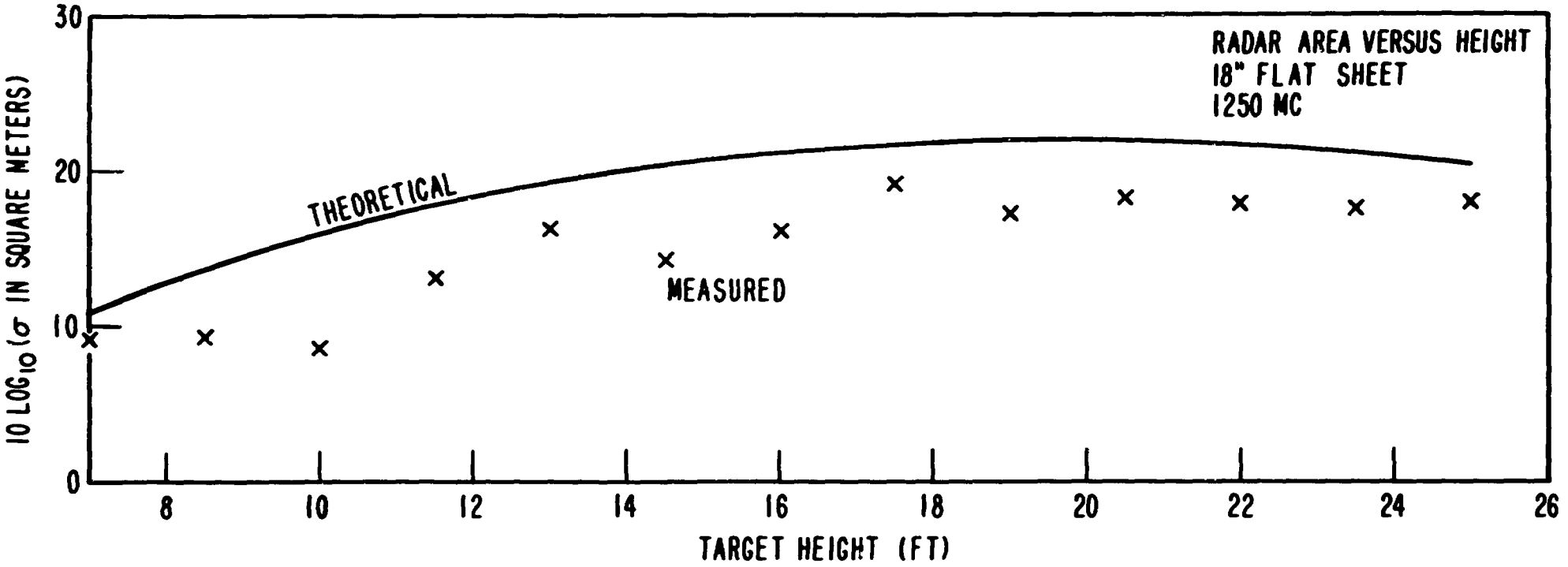
RADAR AREA VERSUS HEIGHT
18" FLAT SHEET
1250 MC
THEORETICAL
MEASURED
10 LOG10 (σ IN SQUARE METERS)
30
20
10
0
8
10
12
14
16
18
20
22
24
26
TARGET HEIGHT (FT)